Published in final edited form as:
Anal Chem. 2008 September 15; 80(18): 6850–6859. doi:10.1021/ac800185x.

Fluorinated Xerogel-Derived Microelectrodes for Amperometric Nitric Oxide Sensing

Jae Ho Shin, **Benjamin J. Privett**, **Justin M. Kita**, **R. Mark Wightman**, and **Mark H. Schoenfisch***
Department of Chemistry, University of North Carolina at Chapel Hill, Chapel Hill, North Carolina 27599

Abstract

An amperometric fluorinated xerogel-derived nitric oxide (NO) microelectrode is described. A range of fluorine-modified xerogel polymers were synthesized via the co-hydrolysis and condensation of alkylalkoxy- and fluoroalkoxysilanes. Such polymers were evaluated as NO sensor membranes to identify the optimum composition for maximizing NO permeability while providing sufficient selectivity for NO in the presence of common interfering species. By taking advantage of both the versatility of sol–gel chemistry and the "poly(tetrafluoroethylene) (PTFE)-like" high NO permselective properties of the xerogels, the performance of the fluorinated xerogel-derived sensors was excellent, surpassing all miniaturized NO sensors reported to date. In contrast to previous electrochemical NO sensor designs, xerogel-based NO microsensors were fabricated using a simple, reliable dip-coating procedure. An optimal permselective membrane was achieved by synthesizing xerogels of methyltrimethoxysilane (MTMOS) and 20% (heptadecafluoro-1,1,2,2-tetrahydrodecyl) trimethoxysilane (17FTMS, balance MTMOS) under acid-catalyzed conditions. The resulting NO microelectrode had a conical tip of ~20 μm in diameter and ~55 mm in length, and exhibited sensitivities of 7.91 pA·nM^{-1} from 0.2 to 3.0 nM (R^2 = 0.9947) and 7.60 nA·mM^{-1} from 0.5 to 4.0 μM (R^2 = 0.9999), detection limit of 83 pM (S/N = 3), response time ($t_{95\%}$) of <3 sec, and selectivity ($\log K^{amp}_{NO,j}$) of −5.74, <−6, <−6, <−6, <−6, −5.84, and −1.33 for j = nitrite, ascorbic acid, uric acid, acetaminophen, dopamine, ammonia/ammonium, and carbon monoxide. In addition, the sensor proved functional up to 20 d, maintaining ≥90% of the sensor's initial sensitivity without serious deterioration in selectivity.

INTRODUCTION

Much work has established nitric oxide (NO), a diatomic free radical endogenously produced in the body, as an important bioregulatory agent involved in multiple physiological processes including vasodilation, neurotransmission, angiogenesis, and phagocytosis.[1-4] For example, NO derived from endothelial cells regulates blood flow and pressure, and inhibits platelet activation and aggregation under normal conditions.[5] Neuroglial cells in the brain produce NO as an intercellular messenger to modulate neuronal excitability, synaptic transmission, arousal,

*To whom correspondence should be addressed. schoenfisch@unc.edu.

SUPPORTING INFORMATION AVAILABLE

Electrooxidation scheme of NO on the platinum working electrode; calculation for preparing a standard NO solution; extended electrochemical properties for fluorinated xerogel-derived NO sensors; solid-state ^{29}Si NMR data for fluorinated xerogel materials; degree of condensation and membrane thickness of the xerogel membrane as a function of fluoroalkoxysilane content; NO permeability and selectivity over nitrite as a function of the membrane thickness; effects of platinization on analytical performance of the microelectrode; and, dynamic response and calibration curves for the fluorinated xerogel-derived microelectrode over extended NO concentrations. This material is available free of charge via the Internet http://pubs.acs.org.

and learning and memory mechanisms.[6] Furthermore, NO has been implicated in diverse NO-mediated disease states and pathophysiological disorders including cardiovascular disease, ischemia-reperfusion injury, and tumor progression.[7,8] The importance of NO measurements in further evaluating NO's biological roles and metabolic pathways warrants improved methods for detecting and monitoring this radical molecule.[9-11]

Designing appropriate strategies for measuring NO in physiological milieu is challenging due to sampling constraints associated with measurement in tissue and cells, NO's low concentration (nM – μM), high reactivity with various endogenous components (e.g., free radicals, transition metal ions, and oxygen), and short half-life (typically <10 s).[3,9-12] Most techniques for measuring NO are indirect, relying on the determination of a secondary species such as L-citrulline (i.e., a coproduct of NO synthesis)[13] and nitrite/nitrate (i.e., oxidation products of NO).[14] Such methods often fail to accurately reflect the spatial and temporal distribution of NO in biological environments.

To overcome the drawbacks of indirect detection strategies, NO has been measured directly via chemiluminescence, fluorescence, electron paramagnetic resonance spectroscopy, mass spectroscopy, gas chromatography, and electrochemistry.[9-12,15-19] Of these methods, electrochemistry is the most straightforward for determining the spatial and temporal distribution of NO at or near its physiological sources.[18-20] In addition to providing direct, real-time monitoring of NO, electrochemical sensors are readily miniaturized, enabling the fabrication of inexpensive microelectrode devices.[18-20] With respect to measuring NO in biological media, the most common electrochemical approaches are based on the direct or catalytic electrooxidation of NO.[18-21] The first successful NO sensor based on the direct electrooxidation of NO was reported by Shibuki using a miniature Clark-style electrode.[22] The electrode was fabricated by placing the working (platinum) and reference (silver) electrodes into a micropipette filled with an internal electrolyte solution. The micropipette was then sealed with a chloroprene gas-permeable membrane (tip diameter of 250 μm). Because the direct electrooxidation of NO requires a relatively high working potential (+0.7 to +1.0 V vs Ag/AgCl), the amperometric detection of NO may be hindered by interference from other readily oxidizable biological species including nitrite, ascorbic acid, uric acid, acetaminophen, and dopamine.[18-22]

In 1992 Malinski and Taha reported the development of an amperometric NO sensor based on NO's electrocatalytic oxidation at a nickel porphyrin-modified carbon electrode.[23] Several metalloporphyrins,[24,25] metal phthalocyanines,[26,27] and other organometallic compounds[28,29] with Ni, Fe, Co, Cu, and Mn centers have been employed to lower the oxidation potential of NO at both carbon and metal (e.g., platinum and gold) electrodes. Bare electrodes are modified via electrochemical polymerization by entrapping the catalytic compounds during the polymerization of a given monomer or using monomers that have covalently linked electrocatalysts.[18-29] The surface-modified electrodes require further modification with a permselective membrane (e.g., Nafion) to reduce interferences by size exclusion and/or electrostatic repulsion.[18-29] Despite significant advances in sensor design, the analytical utility of such electrochemical NO sensors for biological applications remains rather limited due to low sensitivity, lack of sensor specificity, slow response times relative to the rate of physiological changes in NO levels, and/or difficulties in sensor miniaturization.

To facilitate the fabrication of NO microsensors, other polymeric materials have been evaluated as NO-permeable and permselective membranes including polycarbazole,[30] collodion,[31] Nafion,[32,33] *o*- and *m*-phenylenediamine,[34,35] polyeugenol,[36] cellulose acetate,[37,38] poly (tetrafluoroethylene) (PTFE),[39-41] polydimethylsiloxane (silicone rubber),[42,43] and multilayer hybrids[31,44,45] of these polymers. It is well known that amorphous, hydrophobic fluoropolymers are highly permeable to many gaseous species (e.g., oxygen, carbon dioxide,

ammonia, and volatile organic compounds).[46-48] Recently, Meyerhoff and coworkers reported on an improved planar Clark-style NO sensor using a microporous PTFE gas-permeable membrane.[40,41] The PTFE membrane discriminated against potentially interfering species (e.g., nitrite and ascorbic acid) while enabling high NO permeation. However, the fabrication of such sensors remains complicated. For example, the PTFE film must be stretched across the electrode and fixed to the sensor. This process is often irreproducible, impacting both the thickness of the gas-permeable membrane and sensor response to NO.[40,41]

Organically-modified xerogels prepared via the sol–gel process have emerged as a class of polymers suitable for various sensing applications due to (1) mild synthetic conditions, (2) chemical flexibility, (3) versatility (e.g., strong adhesion to a variety of metal/metal oxide substrates), and (4) excellent physical and chemical stability.[49-51] Lev et al. demonstrated the particular benefits of using organically-modified xerogels for oxygen and carbon dioxide gas sensing applications.[52,53] The organically-modified hybrid materials were characterized by an open, rigid structure that allowed for rapid diffusion of gaseous molecules while inhibiting leaching of the internal electrolyte. We previously explored the use of amine-functionalized xerogels as gas-permeable membranes to fabricate amperometric NO microsensors with excellent sensitivity (detection limit of 25 nM) and selectivity ($\log K^{amp}_{NO,j}$ of ca. −6 for j = nitrite, ascorbic acid, uric acid, and acetaminophen).[54]

Despite the unique advantages of using amine-modified xerogels for preparing amperometric NO sensors,[54] their utility as NO-permselective membranes remains hindered due to low permeability to NO, resulting in limited sensitivity to NO at sub-micromolar levels. To reliably assess spatiotemporal dynamics of NO released from single cells, a strong demand for NO sensors sensitive to nanomolar concentrations of NO exists. Herein, we report the synthesis and characterization of a new class of sol–gel derived materials modified with fluorinated functional groups. By taking advantage of both the versatility of sol–gel chemistry and “PTFE-like” high NO permselectivity, the next generation of amperometric NO-selective microelectrodes is fabricated.

EXPERIMENTAL SECTION

Reagents and Materials

Hydrofluoric acid (48 wt % in water) and uric acid were purchased from Aldrich (Milwaukee, WI). (3,3,3-Trifluoropropyl)trimethoxysilane (3FTMS), nonafluorohexyltrimethoxysilane (9FTMS), (tridecafluoro-1,1,2,2-tetrahydrooctyl)trimethoxysilane (13FTMS), and (heptadecafluoro-1,1,2,2-tetrahydrodecyl)trimethoxysilane (17FTMS) were purchased from Gelest (Tullytown, PA). Methyltrimethoxysilane (MTMOS), isobutyltrimethoxysilane (BTMOS), tetramethylsilane (TMS), and tetrabutylammonium chloride were purchased from Fluka (Buchs, Switzerland). Ascorbic acid, acetaminophen, sodium nitrite, dopamine hydrochloride, sodium cholate hydrate, and sodium thiocyanate were purchased from Sigma (St. Louis, MO). An electrocleaning solution (Electrocleaner) was purchased from Shor International (Mt. Vernon, NY). Platinum TP solution (acidic plating solution) was purchased from Technic, Inc. (Cranston, RI). A platinizing solution (3% chloroplatinic acid in water) was purchased from LabChem (Pittsburgh, PA). Silicon (Si) reference/standard solution was purchased from Fisher Scientific (Fair Lawn, NJ). Nitric oxide (NO; 99.5% and 24.1 ppm, balance nitrogen), carbon monoxide (CO; 99.5%), argon (Ar), and nitrogen (N_2) gases were obtained from Linde Gas (Morrisville, NC) or National Welders Supply (Raleigh, NC). Other solvents and chemicals were analytical-reagent grade and used as received. A Millipore Milli-Q UV Gradient A10 System (Bedford, MA) was used to purify distilled water to a final resistivity of 18.2 MΩ cm and a total organic content of ≥6 ppb.

Preparation of Sol–Gel Derived Permselective Membranes

Glass slides were sonicated in ethanol for 20 min, rinsed thoroughly with water, dried with a stream of N_2, and then cleaned in a UV/ozonator (BioForce Nanosciences; Ames, IA) for 20 min prior to modification with xerogel films.[55] Inlaid polycrystalline platinum disk (2-mm diameter) electrodes sealed in Kel-F (total 6-mm diameter; CH Instruments) were mechanically polished with successively finer grades of deagglomerated alumina slurries down to 0.05 μm in particle size (Buehler; Lake Bluff, IL). An ultrasonic cleaner was used to remove residual alumina loosely bound to the surface. The electrodes were then dried with a stream of N_2. A silane solution was prepared by dissolving 45 – 75 μL MTMOS or BTMOS in 300 μL of ethanol. The fluoroalkoxysilane content was varied from 0 to 40% (v/v, balance MTMOS or BTMOS) by the addition of 0 – 30 μL of 3FTMS, 9FTMS, 13FTMS, or 17FTMS for a total silane volume of 75 μL. The silane solutions were mixed with 80 μL of water with or without a catalyst (5 μL of 0.5 M HCl or 0.5 M NaOH) for 1 h (HCl) and 10 min (NaOH), respectively. A shorter period was necessary when using NaOH due to a more rapid gelation rate. The solution was then deposited onto either glass substrates (for material characterization) or Pt working electrodes (0.02, 0.04, 0.07 and 0.11 $\mu L \cdot mm^{-2}$) and allowed to cure for 24 h under ambient conditions. Xerogel film thickness was measured using a Tencor AlphaStep 200 surface profilometer (Brumley South; Mooresville, NC).

Sensor Performance Evaluation

To evaluate the analytical performance of the NO sensors, cyclic voltammetric and amperometric measurements were performed using a CH Instruments 730B bipotentiostat (Austin, TX). The electrode assembly (3-electrode configuration) consisted of a xerogel-modified Pt working electrode (2-mm diameter), a Pt-coiled counter electrode (0.6-mm diameter), and a Ag/AgCl reference electrode (3.0 M KCl; CH Instruments).

Two standard NO solutions (1.9 mM and 41 nM) were prepared by purging phosphate-buffered saline (PBS; 0.01 M, pH 7.4) with Ar for 30 min to remove oxygen, then NO (99.5% and 24.1 ppm) for 30 min. (see Supporting Information for detailed calculations).[31,40] The NO gas was purified before use by passing it through a column packed with KOH pellets to remove trace NO degradation products. The CO solution (0.9 mM) was similarly prepared by successively purging PBS with Ar for 30 min and CO (99.5%) for another 30 min.[56] (Caution! The NO and CO purging process must be carried out in a fume hood since NO and CO gases are toxic!)[45] Solutions of NO and interfering species (e.g., nitrite, ascorbic acid, uric acid, acetaminophen, dopamine, ammonia/ammonium, and carbon monoxide) were prepared fresh every 2 d and stored at 4 °C. All sensors were pre-polarized for at least 30 min and tested in deoxygenated PBS (prepared by purging with N_2) at room temperature with constant stirring. Electrooxidation currents of NO and interfering species were recorded at an applied potential of +0.8 V (vs Ag/AgCl) (see Supporting Information). Sensors were stored in PBS at room temperature between measurements.

To determine the resistance of the xerogel film, AC impedance spectroscopy was performed in PBS (0.01 M, pH 7.4) using a xerogel (10-μm thick)-modified Pt working electrode (2-mm diameter) and a Ag/AgCl reference electrode (3.0 M KCl). A Ensman Instrumentation 400 Potentiostat (Bloomington, IN) was used to apply a 1000 Hz, 20 mV sinusoidal wave to the working electrode. Potentiometry measurements (CH Instruments 730B Biopotentiostat) were also conducted to examine the influence of lipophilic cations and anions on the boundary potential generated at the xerogel/sample interface. The potential between the xerogel-coated Pt and reference electrodes was monitored before and after the addition of lipophilic cations or anions (i.e., tetrabutylammonium, cholate, and thiocyanate) at concentrations up to 1 mM in PBS (0.01 M, pH 7.4).

Xerogel Material Characterization

Xerogel surface wettability was evaluated with a KSV Instruments CAM 200 optical contact angle meter (Helsinki, Finland). The xerogel membranes were spin-coated onto glass slides at a speed of 3000 rpm for 20 s, and allowed to dry for 24 h under ambient conditions. Static water contact angles were obtained as a function of xerogel composition.

To characterize xerogel structural changes, solid-state cross polarization/magic angle spinning (CP/MAS) ^{29}Si nuclear magnetic resonance (NMR) spectra were collected at 20 °C on a Bruker 360 MHz DMX spectrometer (Billerica, MA) equipped with wide-bore magnets (triple axis pulsed field gradient double resonance probes). Xerogel samples were ground, packed into 4 mm zirconia rotors (double resonance frequency of 71.548 MHz), and spun at a speed of 8.0 kHz. The chemical shifts were determined in ppm relative to a TMS external standard. Spectra were deconvoluted by using an OriginPro 7.0 (OriginLab; Northampton, MA), and the peak intensity distributions were fitted to Gaussian functions for T^n where n = 1, 2, and 3 corresponding to the number of siloxane bridges bound to the silicon atom of interest.[57]

Scanning electron microscope (SEM) images of the platinized microelectrode were collected on a Hitachi S4700 field-emission SEM (Tokyo, Japan) using an accelerating voltage of 15 keV (source working distance of 13.5 mm). To obtain high-quality images, samples were coated with a thin layer of gold (ca. 5 nm thickness) using a Cressington 108auto sputter-coater (Watford, England).

Film stability was evaluated by soaking xerogel-coated glass slides in PBS (0.01 M, pH 7.4) at ambient temperature for 1 to 6 weeks. Xerogel fragmentation was determined by measuring the Si concentration in the soak solutions using an ARL-Fisons Spectrascan 7 direct current plasma optical emission spectrometer (DCP-OES; Beverly, MA) (Si detection limit of 0.1 ppm). The instrument was calibrated with 0.0, 1.0, 2.0, 5.0, 10.0, and 25.0 ppm Si standard solutions (PBS). After converting the measured silicon concentration (ppm) to moles, the extent of fragmentation was calculated as a function of exposed xerogel surface area (μmol·cm^{-2}).

Preparation and Evaluation of NO Microelectrodes

For the preparation of platinum microelectrodes (see Figure 1), a tungsten substrate with a diameter of 125 μm and AC resistance of 0.5 MΩ was insulated with parylene-C via a vacuum deposition (A-M Systems; Sequim, WA). The exposed tips (typically 50 – 60 μm length) were cleaned for 10 s in hydrofluoric acid (48 wt % in water), electrolyzed for 30 s at 50 °C in an electrocleaning solution at an applied potential of −5 V (vs a platinum electrode), and rinsed with water.[58] The conical electrode was then transferred into an acidic platinum electroplating solution, plated for 5 s at 50 °C at an applied potential of −0.5 V (vs a platinum electrode), and rinsed with water and ethanol.[57] The ensuing platinum-deposited working electrode was platinized in 3% chloroplatinic acid (v/v in water) by cycling the potential from +0.6 to −0.35 V (vs Ag/AgCl) at a scan rate of 20 mV/sec using a CH Instruments 730B bipotentiostat.[40, 54] Finally, the multilayered microelectrode (i.e., platinum black/platinum/tungsten, Pt-B/Pt/W) was modified with the optimized fluorinated xerogel-derived permselective membrane by dip-coating the sensor tip into a sol solution consisting of 60 μL of MTMOS, 15 μL of 17FTMS, 300 μL of ethanol, 80 μL of water, and 5 μL of 0.5 M HCl. After allowing the xerogel “film” to cure for 10 min, the process was repeated to yield a ~2.5 μm thick final membrane. The xerogel-modified electrode was then allowed to dry for 24 h under ambient conditions.

Response and calibration curves were obtained by injecting aliquots of the standard NO solution (1.9 mM or 41 nM) into 100 mL of PBS (0.01 M, pH 7.4; not deoxygenated) at room temperature under constant stirring. All microelectrodes were pre-polarized for 30 min to 5 h.

Currents were recorded at an applied potential of +0.7 and +0.8 V (vs Ag/AgCl) for the platinized and non-platinized working electrodes, respectively.

RESULTS AND DISCUSSION

Fluorinated Xerogel Sensor Membranes

To determine the feasibility of developing a fluorinated xerogel film for selective amperometric detection of NO, we evaluate the effects of the xerogel composition on its physicochemical properties including hydrophobicity, porosity, and density, all of which ultimately influence sensor performance (e.g., permeability, selectivity, and permselectivity). The structures of the alkylalkoxy- and fluoroalkoxysilanes used in this work (i.e., methyltrimethoxysilane (MTMOS), isobutyltrimethoxysilane (BTMOS), (3,3,3-trifluoropropyl)trimethoxysilane (3FTMS), nonafluorohexyltrimethoxysilane (9FTMS), (tridecafluoro-1,1,2,2-tetrahydrooctyl) trimethoxysilane (13FTMS), and (heptadecafluoro-1,1,2,2-tetrahydrodecyl)trimethoxysilane (17FTMS)) are shown in Figure 2. The permeability of the sol–gel derived films to NO (P^e_{NO}) and nitrite ($P^e_{NO_2^-}$), the most problematic interfering species for NO sensors in biological milieu due to its size similarity, was determined electrochemically by measuring the ratio of peak currents at the xerogel coated (ΔI_x) and bare Pt (ΔI_b) electrodes in 10 μM NO and 100 μM nitrite solutions, respectively.[54,59]

$$P_i^e = \frac{\Delta I_x}{\Delta I_b} \tag{1}$$

The selectivity of the xerogel-modified sensors for NO in the presence of interfering species was also evaluated using the separate solution method,[60] for which the amperometric selectivity coefficients ($\log K^{amp}_{NO,j}$) were calculated using the following equation:

$$\log K^{amp}_{NO,j} = \log\left(\frac{\Delta I_j / c_j}{\Delta I_{NO} / c_{NO}}\right) \tag{2}$$

where ΔI_{NO} and ΔI_j are the measured current values for the target analyte (NO) and interfering species (j = nitrite, ascorbic acid, uric acid, acetaminophen, dopamine, ammonia/ammonium, and carbon monoxide), respectively. The concentration of each interfering substance (c_j) was selected to be 100 μM, 10 times greater than the concentration of NO (c_{NO}). To further evaluate the ability of xerogel films to differentiate NO over nitrite, the ratio of NO and nitrite permeability was used to determine permselectivity (α_{NO,NO_2^-}) according to:[61]

$$\alpha_{NO,NO_2^-} = \frac{P^e_{NO}}{P^e_{NO_2^-}} \tag{3}$$

To identify the optimum xerogel composition, the performance of xerogel-modified NO sensors was first evaluated using macroelectrodes (Pt, 2 mm diameter). Several xerogel films were prepared by combining an alkylalkoxysilane (i.e., MTMOS) with a fluoroalkoxysilane (i.e., 3FTMS, 9FTMS, 13FTMS, or 17FTMS) as potential permselective membranes (Figure 3 and Supporting Information, Table S1). The initial concentration of the fluoroalkoxysilane used to prepare each xerogel was 20% (v/v, balance MTMOS). Our findings illustrate the drastic effects of fluorine derivatization on both the permeability and selectivity of xerogel-derived NO sensors. Unfortunately, the 3FTMS xerogel with highest NO permeability (0.77

of P^{e}_{NO}) was characterized by poorest selectivity (−1.90 of K^{amp}_{NO,NO_2^-}). As the number of fluorine substituents was increased from 3 to 17 (corresponding to 3FTMS to 17FTMS), the selectivity for NO over nitrite was significantly improved (−2.00 to −3.21 of $\log K^{amp}_{NO,NO_2^-}$ and 4.1 to 83 of α_{NO,NO_2^-}, respectively). Furthermore, the NO permeability increased from 0.2 to 0.75 with increasing the degree of fluorination in the silane structure from 9FTMS to 17FTMS. Such behavior was surprising since glassy and rubbery polymers previously used as permselective membranes for sensor and separation applications exhibited a tradeoff between permeability and selectivity.[62] For example, films with high permeability were characterized by poor selectivity and vice versa.

The unexpected trends in permeability and selectivity may result from changes in the hydrophobicity of the xerogel matrix. Indeed, it is well known that NO is non-polar, an attribute critical to its physiological function, permitting this small molecule to pass readily across hydrophobic cell membrane boundaries.[63] The hydrophobicity of the permselective films would thus be beneficial for enhancing NO permeation,[26,54] while effectively rejecting the diffusion of ionic, hydrophilic interfering species such as nitrite, ascorbic acid, uric acid, and dopamine. Static water contact angle measurements were employed to assess the surface wettability of fluorinated xerogels prepared with different types of fluoroalkoxysilanes (Figure 4). As expected, the increase in the degree of fluorination from 3FTMS to 17FTMS resulted in a concomitant increase in surface hydrophobicity of the xerogel membranes from 85.3 ± 1.7 to 104.1 ± 0.6°. 17FTMS-modified xerogels, characterized as having the most ideal correlation between permeability and selectivity, were thus chosen for subsequent experiments.

The sensor performance of 17FTMS/MTMOS xerogels was further manipulated by varying the catalytic conditions during xerogel polymerization. As shown in Table 1, using an acid catalyst (6.5 mM HCl) was more effective for preparing the 17FTMS/MTMOS xerogel than no catalyst or a base catalyst (6.5 mM NaOH). Indeed, sensors fabricated using 20% 17FTMS/MTMOS xerogel membranes synthesized under acid-catalyzed conditions were characterized by ca. 2 orders of magnitude greater NO selectivity over nitrite (i.e., −5.74 of $\log K^{amp}_{NO,NO_2^-}$ and 7200 of $\alpha_{NO,\,NO_2^-}$ compared to controls, without significant deterioration in permeability to NO (0.72 of P^{e}_{NO}). In contrast, the NO permeability for xerogel membranes prepared under base-catalyzed conditions was significantly compromised (0.13 of P^{e}_{NO}). This result may be attributed to structural changes (e.g., porosity and density) in the xerogel networks.

To understand the influence of the catalytic conditions on xerogel structure, solid-state ^{29}Si NMR spectra were collected for 20% 17FTMS (balance MTMOS) prepared with and without catalysts. Cross polarization and magic angle spinning (CP/MAS) NMR techniques were employed to increase the signal resolution and sensitivity of the silicon atoms in proximity to protons.[57,64,65] The NMR spectra for 20% 17FTMS xerogels (balance MTMOS) synthesized without (control) and with catalyst (i.e., acidic and basic) are shown in Figure 5. (The relative intensities of peaks are provided in Supporting Information, Table S2.) Three distinct peaks were observed in the ^{29}Si NMR spectra of the fluoroalkoxysilane-modified xerogels indicating three distinct silicon chemical environments. Traditionally, the peaks at chemical shifts of approximately −44, −53, and −62 ppm are representatives of silicon atoms connected to T^1 (geminal silanol; $-OSi(OH)_2R$), T^2 (single silanol; $-O_2Si(OH)R$), and T^3 (siloxane; $-O_3SiR$) structures, respectively, where R is a alkyl or fluoroalkyl group (Figure 5B).[56,63] The presence of T^n bands suggests covalent linkages between the organic group and the xerogel backbone (i.e., Si–C bridges).

The addition of 6.5 mM HCl or NaOH to the sol resulted in xerogels characterized by reduced relative intensities of the T^1 and T^2 peaks and an accompanying increase in the intensity of the

T^3 peak. The density of the silica networks was determined by calculating the degree of condensation (%*DC*) according to the following equation:[66]

$$\%DC = \frac{\sum_n nq^n}{f} = \frac{\sum_{n=1}^{3} nI(T^n)}{3} \quad (4)$$

where q^n represents the relative intensity (I) of the T^n species, and f refers to the connectivity of the silane monomer, determined by the number of reactive alkoxy sites (i.e., $f = 3$ for T^n structures). The %*DC* of 17FTMS xerogels prepared under acid- and base-catalyzed conditions increased to 86.4 ± 1.1 and 90.2 ± 1.3, respectively, indicating the synthesis of more dense xerogels versus control (no catalyst, %*DC* = 78.3 ± 1.2). Of note, the quantitative analysis of these structures is complicated because the intensity of each peak depends on the efficiency of cross polarization and proton relaxation time.[49] Our previous work demonstrated that control over the porosity and density of the xerogel matrix is vital for optimizing the selectivity of NO sensors without compromising NO permeability.[54] As such, xerogel sensor membranes prepared under base-catalyzed conditions result in xerogel structures that are too dense for sensor use, disrupting the diffusion of NO through the membrane.

To evaluate the effect of varying the xerogel fluoroalkoxysilane concentration on membrane permeability and sensor performance, the relative concentration of 17FTMS used to prepare the membrane was varied from 10 to 40% (balance MTMOS). Based on the catalyst study, xerogel films were synthesized under acid-catalyzed conditions (6.5 mM HCl) to enhance the polycondensation of the xerogel network. As shown in Figure 6, electrodes modified with a 20% 17FTMS xerogel membrane were characterized by the highest NO permeability and most effective discrimination over nitrite (i.e., 0.72 of P^e_{NO}, −5.74 of $\log K^{amp}_{NO,NO_2^-}$, and 7200 of α_{NO,NO_2^-}, respectively). The trends in permeability and selectivity with increasing 17FTMS concentration may be the result of multiple subtle changes in the physicochemical properties of the xerogel including the hydrophobicity, degree of condensation, and membrane thickness. As shown in Figure 7, increasing the 17FTMS concentration of the sol from 0 to 20% (balance MTMOS) resulted in more hydrophobic xerogels (75.2 ± 1.2 to 100.0 ± 0.7°). However, the hydrophobicity of xerogels prepared using 17FTMS concentrations >20% did not continue to increase, indicating that the enhanced NO permeability was not solely linked to the surface energy of the membrane. In contrast, as the concentration of 17FTMS was increased from 20 to 40%, both the degree of condensation and the membrane thickness increased slightly from 86.4 ± 1.1 to 87.6 ± 1.0 and 9.6 ± 0.41 to 11.7 ± 0.25 μm, respectively (Supporting Information, Figure S1).

To identify the optimum membrane thickness for maximizing permeability without compromising sensor selectivity, the thickness of 20% 17FTMS xerogels synthesized under acid-catalyzed conditions was varied. Electrodes coated with 0.02, 0.04, 0.08, and 0.12 $\mu L \cdot mm^{-2}$ of the sol solution resulted in membrane thicknesses of 7.8, 9.6, 10.9, and 13.5 mm, respectively. The 7.8- and 9.6-μm-thick membranes exhibited greater NO permeability than the 10.9- and 13.5-μm thick membranes (Supporting Information, Figure S2). The thinnest membrane (7.8 μm) was characterized by poor selectivity over nitrite. The optimum xerogel membrane thickness was thus determined to be 9.6 μm since this film demonstrated the best compromise in permeability to NO and selectivity over nitrite. In an attempt to further enhance the xerogel hydrophobicity, BTMOS, an alkylalkoxysilane with a longer alkyl chain compared to MTMOS (i.e., butyl vs methyl) was employed as the backbone silane. Unfortunately, BTMOS-based xerogels proved to be unstable in aqueous media. Based on the above results, a 9.6-μm thick acid-catalyzed 20% 17FTMS/MTMOS xerogel film was determined to be the optimum membrane for fabricating a xerogel-based NO sensor. Indeed, the NO permeability

and selectivity ($\log K^{amp}_{NO,j}$) of 17FTMS/MTMOS-modified sensors were 0.72 and −5.74, <−6, <−6, <−6, <−6, −5.84, and −1.33 for *j* = nitrite, ascorbic acid, uric acid, acetaminophen, dopamine, ammonia/ammonium, and carbon monoxide, respectively. The use of the fluorinated xerogel membranes improved the NO permeability >7-fold compared to previously reported aminoalkoxysilane-derived xerogel sensors. In addition, sensors coated with the "PTFE-like" xerogel films did not exhibit serious interference towards ammonia/ammonium, in contrast to sensors employing PTFE gas-permeable membranes.[41] Cha and Meyerhoff reported ammonia as an additional interfering species for the measurement of NO in physiological fluids.[41] At neutral pH, ca. 1% of total ammonia (i.e., ammonia/ammonium, pKa 9.25) exists in the form of dissolved ammonia gas, which may be electrochemically oxidized at the surface of several metal catalysts including platinized platinum.[41,67] In contrast, amperometric NO sensors using porous PTFE as NO-permeable membranes exhibited poor selectivity over total ammonia (i.e., −3.1 and −1.1 of $\log K^{amp}_{NO,j}$, *j* = ammonium and ammonia, respectively).[41]

Although the mechanism by which current is carried through the fluorous xerogel is not definitive at this time, the resistance of the xerogel membrane was low (ca. 2.75 Ωk for 10-μm films as measured via AC impedance). Such a low resistance would be expected based on the quality of the sensor response to NO. Potentiometry measurements were also conducted to evaluate the influence of lipophilic cations and anions on the boundary potential generated at the xerogel/sample interface. The generation of a boundary potential at the xerogel surface would likely alter the applied potential during amperometric measurements resulting in erratic signal. Changes in the potential were thus monitored before and after the addition of lipophilic cations or anions (e.g., tetrabutylammonium, cholate, and thiocyanate) to the sample solution. Even at concentrations up to 1 mM, such cations and anions did not significantly alter the electrode potential.

Xerogel Material Stability

The stability of the sol–gel derived coatings under physiological conditions is a critical consideration for the development of in vivo NO sensors. Fragmentation of the xerogel due to swelling and/or cracking may present serious toxicity concerns and lead to loss of sensor function. To assess material stability, xerogel films prepared with the aforementioned optimized composition (20% 17FTMS, balance MTMOS) were cured for 24 h under ambient conditions, and immersed in PBS (pH 7.4) at room temperature for up to 6 weeks. At regular intervals, the extent of xerogel fragmentation was determined by measuring the concentration of silicon in the soak solution via DCP-OES analysis.

As shown in Table 2, 20% 17FTMS/MTMOS films synthesized under acid-catalyzed conditions exhibited minimal xerogel fragmentation, with measured silicon values below 0.04 μmol·m^{-2} up to 2 weeks. While slight xerogel fragmentation was observed at longer soak times, the fluorinated xerogel coatings remained stable with a maximum measurable fragmentation of only 0.20 ± 0.08 μmol·cm^{-2} Si at 6 weeks. Previous studies have indicated that the stability of the xerogel films is significantly affected by both the type and amount of organosilanes used to prepare the sol.[54,68] Of the xerogel combinations used to develop NO-permselective membranes, 20% (aminoethylaminomethyl)phenethyltrimethoxysilane (AEMP3) (balance MTMOS) proved to be the most stable xerogel formulation with fragmentation of 0.61 ± 0.08 μmol·cm^{-2} Si at 10 d.[54] Of note, the remarked improved stability for fluorine-modified xerogel coatings relative to AEMP3-based xerogels is attributed to a higher degree of condensation for the xerogel matrix, indicating that the presence of the bulky fluorinated group (i.e., heptadecafluoro-1,1,2,2-tetrahydrodecyl) does not significantly compromise the stability of the resulting xerogel networks.

Microelectrodes for Amperometric Detection of NO

A microelectrode for selective detection of NO was fabricated by first electrodepositing platinum on a tapered tungsten wire that was insulated with a parylene-C polymer (Figure 1). Before modifying the exposed tip (~50 – 60 μm in length) of the conical Pt/W wire with the xerogel permselective membrane, the surface of the Pt/W electrode was platinized, resulting in the deposition of platinum black (Pt-B) on the Pt/W electrode. Platinized Pt electrodes have been widely utilized to devise chemical and biological voltammetric/amperometric sensors with improved response characteristics.[40,69] To assess the influence of platinization on the electrochemical oxidation of NO, cyclic voltammetry and amperometry were carried out at both control Pt/W and platinized Pt/W working electrodes (Supporting Information, Figures S3 and S4). As expected, the current changes observed from the voltammograms were significantly greater (~17 times after background correction) for the platinized Pt/W electrodes compared to control Pt/W electrodes. The improved signal may be attributed to increases in the effective surface area of the electrode and faster electron-transfer kinetics for NO. Similarly, the amperometric sensitivity of the platinized electrodes was roughly 20 times greater than that of the non-platinized electrodes (i.e., 0.38 vs 7.38 $nA \cdot \mu M^{-1}$) at an applied potential of +0.8 and +0.7 V vs Ag/AgCl for the non-platinized and platinized Pt electrodes, respectively. All subsequent experiments were conducted with platinized Pt/W microelectrodes.

The platinized Pt/W microelectrode was modified with the optimized fluorinated xerogel NO-permselective membrane by immersing the tip of the electrode into a sol solution consisting of 60 μL of MTMOS, 15 μL of 17FTMS (20%, balance MTMOS), 300 μL of ethanol, 80 μL of water, and 5 μL of 0.5 M HCl. (A final membrane thickness of ~9.5 μm was achieved by repeating this procedure.) The analytical performance of the resulting NO microelectrode was then investigated. The calibration and dynamic response curves for NO and various interfering species (e.g., nitrite, ascorbic acid, uric acid, acetaminophen, dopamine, and ammonia/ammonium) are shown in Figure 8. The concentration of each interfering substance was chosen to be greater than the highest level that would be present in a physiological sample (i.e., 100 μM each of nitrite, ascorbic acid, uric acid, acetaminophen, dopamine, and ammonia/ammonium). Employing the fluorinated xerogel (i.e., 20% 17FTMS/MTMOS prepared under acid-catalyzed conditions) permselective membrane allowed for the development of NO microelectrodes with remarkably improved sensor performance, surpassing all miniaturized NO sensors reported to date with respect to sensitivity (7.91 ± 0.95 $pA \cdot nM^{-1}$), linearity (R^2 = 0.9947, 0.2 – 3.0 nM NO range), detection limit (83 pM, based on S/N = 3), and response time ($t_{95\%}$ = typically <3 s).[18,19,54] Furthermore, the xerogel-derived sensor responded linearly to NO up to 4 μM (7.60 $nA \cdot \mu M^{-1}$, R^2 = 0.9999; Supporting Information, Figure S5).

The response variations of the fluorinated xerogel-derived NO microsensors to NO (in the range of 0.2 – 3.0 nM) and multiple interfering species as a function of time are shown in Figure 9. With respect to stability, the sensor retained 95% of its initial sensitivity at 6 d. Even after 20 d, 90% of the sensor's initial response (sensitivity) was maintained when soaked continuously in PBS at room temperature. Furthermore, the selectivity (total interference response) of the sensor did not change as a function of soak time, indicating that significant structural changes (i.e., membrane porosity and density) did not occur up to 25 d. The gradual decrease in NO sensitivity at periods >25 d is likely due to the accumulation of nitrate (NO_3^-) produced by the electrochemical oxidation of NO within the gap between the electrode surface and the membrane, and/or hydration of the xerogel film. Hydration of the fluorinated membrane would impact the xerogel hydrophobicity, eventually decreasing both analyte permeability and sensor selectivity.

CONCLUSION

The use of fluorinated xerogel-derived permselective membranes for developing ultrahigh sensitive, NO microsensors enables the measurement of NO at sub-nanomolar concentrations in the presence of common biological interfering species. Several xerogel films were fabricated by varying the type and amount of alkylalkoxy- and fluoroalkoxysilane precursors, and the catalytic conditions during the sol–gel polymerization to identify an optimum membrane composition. In contrast to previous sensor designs for electrochemical NO measurements, the fabrication of NO microsensors via sol–gel chemistry is significantly more straightforward. Indeed, xerogel-based NO microsensors prepared via a simple dip-coating procedure are characterized by outstanding sensitivity (7.91 pA·nM^{-1} from 0.2 to 3.0 nM, R^2 = 0.9947; and 7.60 nA·μM^{-1} from 0.5 to 4.0 μM, R^2 = 0.9999), detection limit (83 pM), selectivity (−5.74, <−6, <−6, <−6, <−6, −5.84, and −1.33 of $\log K^{amp}_{NO,j}$, j = nitrite, ascorbic acid, uric acid, acetaminophen, dopamine, ammonia/ammonium, and carbon monoxide, respectively), response time ($t_{95\%}$ = <3 s), and lifetime (20 d retaining 90% of the sensor's initial response). Future studies aim to employ the NO microelectrodes developed herein for in situ and in vivo measurements of NO in the single cells and brain tissue.

Supplementary Material

Refer to Web version on PubMed Central for supplementary material.

Acknowledgments

This research was supported by the National Institutes of Health (NIH EB000708 for M.H.S. and NIH DA10900 for R.M.W.).

REFERENCES

1. Ignarro LJ, Bugga GM, Wood KS, Byrns RE, Chaudhuri G. Proc. Natl. Acad. Sci. U.S.A 1987;84:9265–9269. [PubMed: 2827174]
2. Moncada S, Higgs A. N. Engl. J. Med 1993;30:2002–2011. [PubMed: 7504210]
3. Ignarro, LJ. Nitric Oxide: Biology and Pathobiology. Academic Press; San Diego: 2000.
4. Butler, AR.; Nicholson, R. Life, Death and Nitric Oxide. Royal Society of Chemistry; Cambridge: 2003.
5. Radomski MW, Palmer RMJ, Moncada S. Br. J. Pharmacol 1987;92:639–646. [PubMed: 3322462]
6. Moncada S, Palmer RMJ, Higgs EA. Pharmacol. Rev 1991;43:109–142. [PubMed: 1852778]
7. Napoli C, Ignarro LJ. Annu. Rev. Pharmacol. Toxicol 2003;43:97–123. [PubMed: 12540742]
8. Keefer LK. Annu. Rev. Pharmacol. Toxicol 2003;43:585–607. [PubMed: 12415121]
9. Archer S. FASEB J 1993;7:349–360. [PubMed: 8440411]
10. Yao D, Vlessidis AG, Evmiridis NP. Microchim. Acta 2004;147:1–20.
11. Bryan NS, Grisham MB. Free Radical Biol. Med 2007;43:645–657. [PubMed: 17664129]
12. Beckman, JS.; Wink, DA.; Crow, JP. Methods in Nitric Oxide Research. Feelisch, M.; Stamler, JS., editors. John Wiley; Chichester, U.K.: 1996. Chapter 6
13. Guthohrlein G, Knappe J. Anal. Biochem 1968;26:188–191. [PubMed: 5758029]
14. Griess JP. Ber. Dtsch. Chem. Ges 1879;12:426–429.
15. Robinson JK, Bollinger MJ, Birks JW. Anal. Chem 1999;71:5131–5136. [PubMed: 10575964]
16. Gomes A, Fernandes E, Lima JLFC. J. Fluorescence 2006;16:119–139.
17. Lim MH, Lippard SJ. Acc. Chem. Res 2007;40:41–51. [PubMed: 17226944]
18. Bedioui F, Villeneuve N. Electroanalysis 2003;15:5–18.
19. Ciszewski A, Milczarek G. Talanta 2003;61:11–26. [PubMed: 18969158]
20. Zhang X. Front. Biosci 2004;9:3434–3446. [PubMed: 15353368]

21. de Vooys ACA, Beltramo GL, van Riet B, van Veen JAR, Koper MTM. Electrochim. Acta 2004;49:1307–1314.
22. Shibuki K. Neurosci. Res 1990;9:69–76. [PubMed: 2175870]
23. Malinski T, Taha Z. Nature 1992;358:676–678. [PubMed: 1495562]
24. Diab N, Schuhmann W. Electrochim. Acta 2001;47:265–273.
25. Oni J, Diab N, Reiter S, Schuhmann W. Sens. Actuators B 2005;105:208–213.
26. Pontie M, Gobin C, Pauporte T, Bedioui F, Devynck J. Anal. Chim. Acta 2000;411:175–185.
27. Pereira-Rodrigues N, Albin V, Koudelka-Hep M, Auger V, Pailleret A, Bedioui F. Electrochem. Commun 2002;4:922–927.
28. Casero E, Pariente F, Lorenzo E, Beyer L, Losada J. Electroanalysis 2001;13:1411–1416.
29. Mori V, Toledo JC, Silva HAS, Franco DW, Bertotti M. J. Electroanal. Chem 2003;547:9–15.
30. Prakash R, Srivastava RC, Seth PK. Polym. Bull 2001;46:487–490.
31. Kitamura Y, Uzawa T, Oka K, Komai Y, Takizawa N, Kobayashi H, Tanishita K. Anal. Chem 2000;72:2957–2962. [PubMed: 10905334]
32. Zhang X, Cardosa L, Broderick M, Fein H, Lin J. Electroanalysis 2000;12:1113–1117.
33. Kashevskii AV, Safronov AY, Ikeda O. J. Electroanal. Chem 2001;510:86–95.
34. Friedemann MN, Robinson SW, Gerhardt GA. Anal. Chem 1996;68:2621–2628. [PubMed: 8694261]
35. Park J-K, Tran PH, Chao JKT, Ghodadra R, Rangarajan R, Thakor NV. Biosens. Bioelectron 1998;13:1187–1195. [PubMed: 9871974]
36. Ciszewski A, Milczarek G. Electroanalysis 2001;13:860–867.
37. Pallini M, Curulli A, Amine A, Palleschi G. Electroanalysis 1998;10:1010–1016.
38. Cserey A, Gratzl M. Anal. Chem 2001;73:3965–3974. [PubMed: 11534724]
39. Do J-S, Wu K-J, Tsai M-L. Sens. Actuators B 2002;86:98–105.
40. Lee Y, Oh BK, Meyerhoff ME. Anal. Chem 2004;76:536–544. [PubMed: 14750844]
41. Cha W, Meyerhoff ME. Chem. Anal 2006;51:949–961.
42. Mizutani F, Yabuki S, Sawaguchi T, Hirata Y, Sato Y, Iijima S. Sens. Actuators B 2001;76:489–493.
43. Kato D, Sakata M, Hirayama C, Hirata Y, Mizutani F, Kunitake M. Chem. Lett 2002:1190–1191.
44. Katrlik J, Zalesakova P. Bioelectrochemistry 2002;56:73–76. [PubMed: 12009447]
45. Zhang X, Lin J, Cardoso L, Broderick M, Darley-Usmar V. Electroanalysis 2002;14:697–703.
46. Hitchman, ML. Measurement of Dissolved Oxygen. John Wiley and Sons; New York: 1978.
47. Su X-L, Yu B, Tan H, Yang X, Nie L, Yao S. J. Pharm. Biomed. Anal 1998;16:759–769. [PubMed: 9535187]
48. Moskvin LN, Nikitina TG. J. Anal. Chem 2004;59:2–16.
49. Hench LL, West JK. Chem. Rev 1990;90:33–72.
50. Walcarius A. Electroanalysis 1998;10:1217–1235.
51. Walcarius A. Chem. Mater 2001;13:3351–3372.
52. Tsionsky M, Lev O. Anal. Chem 1995;67:2409–2414.
53. Rabinovich L, Lev O, Tsirlina GA. J. Electroanal. Chem 1999;466:45–59.
54. Shin JH, Weinman SW, Schoenfisch MH. Anal. Chem 2005;77:3494–3501. [PubMed: 15924380]
55. Robbins ME, Oh BK, Hopper ED, Schoenfisch MH. Chem. Mater 2005;17:3288–3296.
56. Lee Y, Kim J. Anal. Chem 2007;79:7669–7675. [PubMed: 17877421]
57. Albert K, Bayer E. J. Chromatogr 1991;544:345–370.
58. Hermans A, Wightman RM. Langmuir 2006;22:10348–10353. [PubMed: 17129002]
59. Shin JH, Marxer SM, Schoenfisch MH. Anal. Chem 2004;76:4543–4549. [PubMed: 15283600]
60. Stefan, R-I.; van Staden, JF.; Aboul-Enein, HY. Electrochemical Sensors in Bioanalysis. Marcel Dekker; New York: 2001.
61. Cruz J, Kawasaki M, Gorski W. Anal. Chem 2000;72:680–686. [PubMed: 10701250]
62. Dai Y, Guiver MD, Robertson GP, Kang YS, Lee KJ. Macromolecules 2003;36:6807–6816.
63. Bonner, FT.; Stedman, G. Methods in Nitric Oxide Research. Feelisch, M.; Stamler, JS., editors. John Wiley; Chichester, U.K.: 1996. Chapter 1

64. Huh S, Wiench JW, Yoo J-C, Pruski M, Lin VS-Y. Chem. Mater 2003;15:4247–4256.
65. Bruch MD, Fatunmbi HO. J. Chromatogr. A 2003;1021:61–70. [PubMed: 14735975]
66. Armelao L, Gross S, Muller K, Pace G, Tondello E, Tsetsgee O, Zattin A. Chem. Mater 2006;18:6019–6030.
67. de Moshima BAL, Lescano D, Holgado TM, Mishima HT. Electrochim. Acta 1998;43:395–404.
68. Marxer SM, Rothrock AR, Nablo BJ, Robbins ME, Schoenfisch MH. Chem. Mater 2003;15:4193–4199.
69. Feltham AM, Spiro M. Chem. Rev 1971;71:177–193.

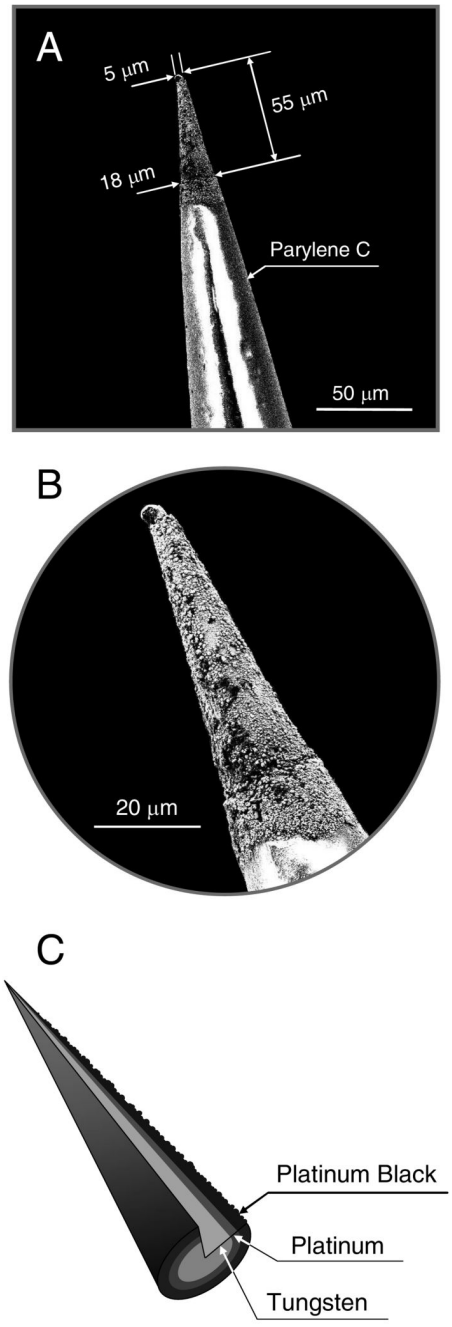

Figure 1.
(A) SEM image of a conical microelectrode fabricated by consecutive electrodepositions of platinum and platinum black on a tungsten substrate (Pt-B/Pt/W); (B) Magnified view of the conical tip of the Pt-B/Pt/W microelectrode shown in (A); and, (C) Schematic illustrating the multilayered structure of platinum and platinum black deposited on the tapered tungsten wire.

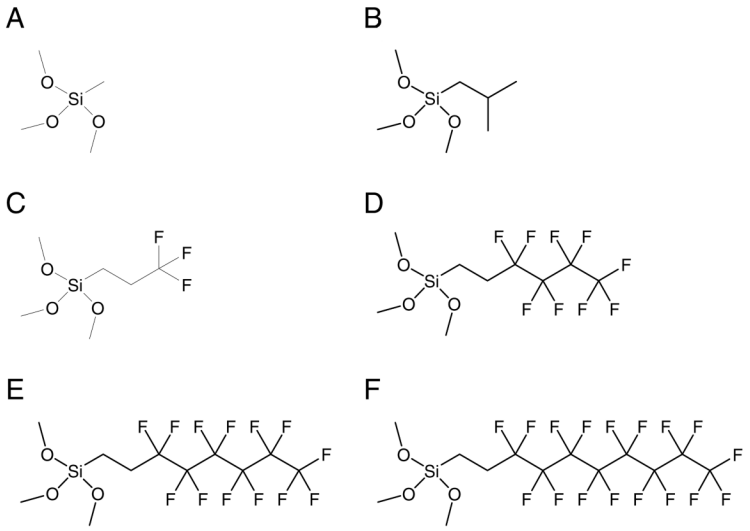

Figure 2.

Structures of alkylalkoxy- and fluoroalkoxysilanes used in this work: (A) methyltrimethoxysilane (MTMOS); (B) isobutyltrimethoxysilane (BTMOS); (C) trifluoropropyltrimethoxysilane (3FTMS); (D) nonafluorohexyltrimethoxysilane (9FTMS); (E) (tridecafluoro-1,1,2,2-tetrahydrooctyl)-trimethoxysilane (13FTMS); and, (F) (heptadecafluoro-1,1,2,2-tetrahydrodecyl)trimethoxysilane (17FTMS).

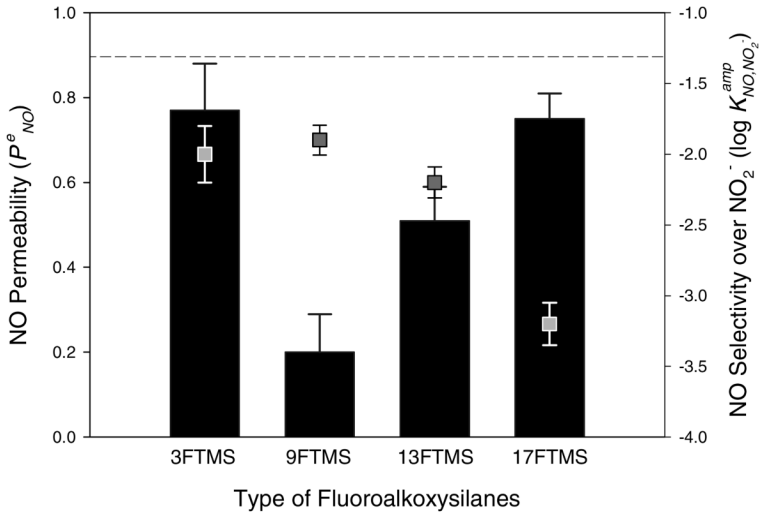

Figure 3.

NO permeability (bar graphs, left axis) and selectivity over nitrite (scatter plots, right axis) as a function of the type of fluoroalkoxysilanes (20%, balance MTMOS). The dashed line indicates NO selectivity of the bare Pt electrode over nitrite. Data are represented as means ± SD (*n* is at least 3).

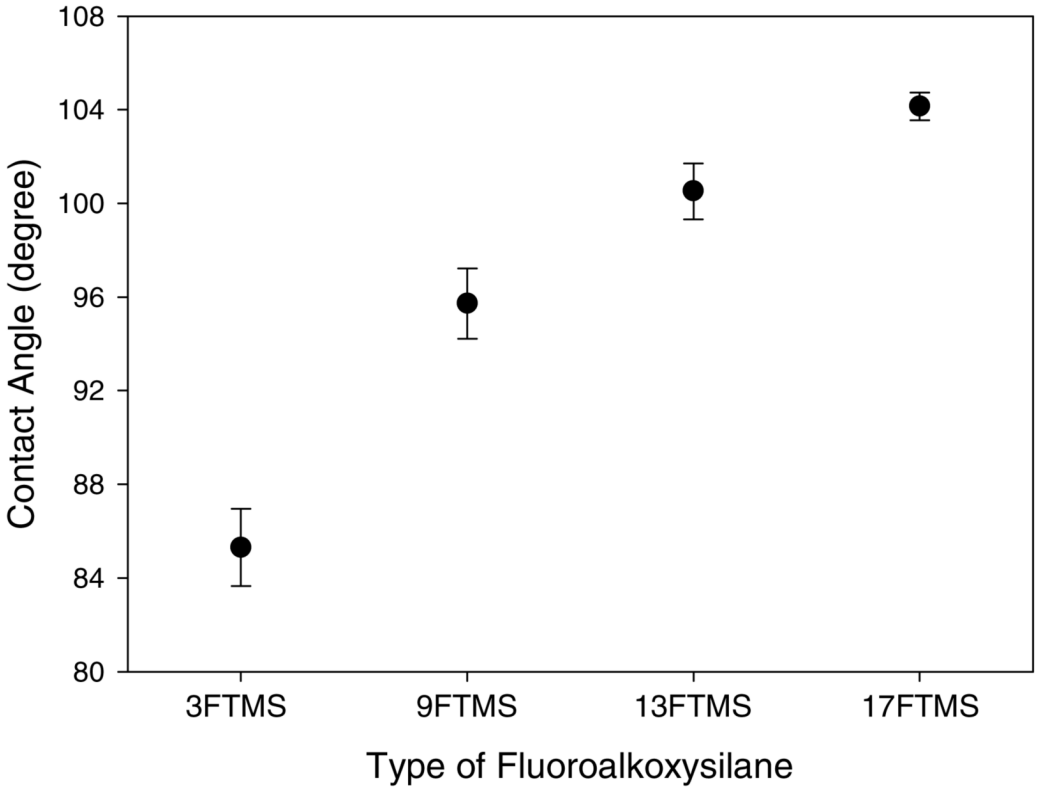

Figure 4.
Static water contact angles as a function of the type of fluoroalkoxysilanes (20%, balance MTMOS). Data are represented as means ± SD (n = 15).

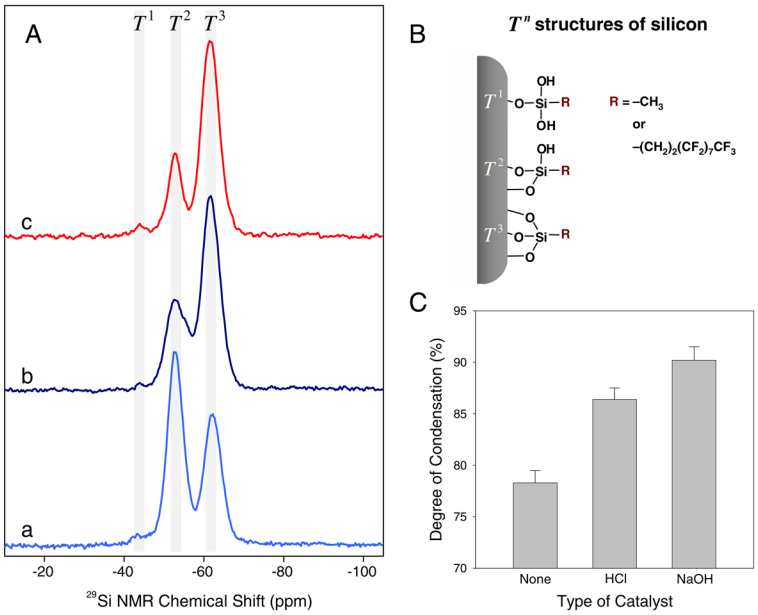

Figure 5.

(A) Solid-state ^{29}Si CP/MAS NMR spectra of 20% 17FTMS xerogel materials (balance MTMOS) synthesized under different catalytic conditions: (a) no catalyst, (b) acidic (6.5 mM HCl), and (c) basic catalysts (6.5 mM NaOH). (B) Schematic illustrating silicon chemical environments of 17FTMS/MTMOS xerogels. (C) Degree of condensation (%DC) of fluorinated xerogel films (20% 17FTMS, balance MTMOS) as a function of catalytic conditions during the xerogel polymerization. The data are represented as means ± SD (*n* is at least 3).

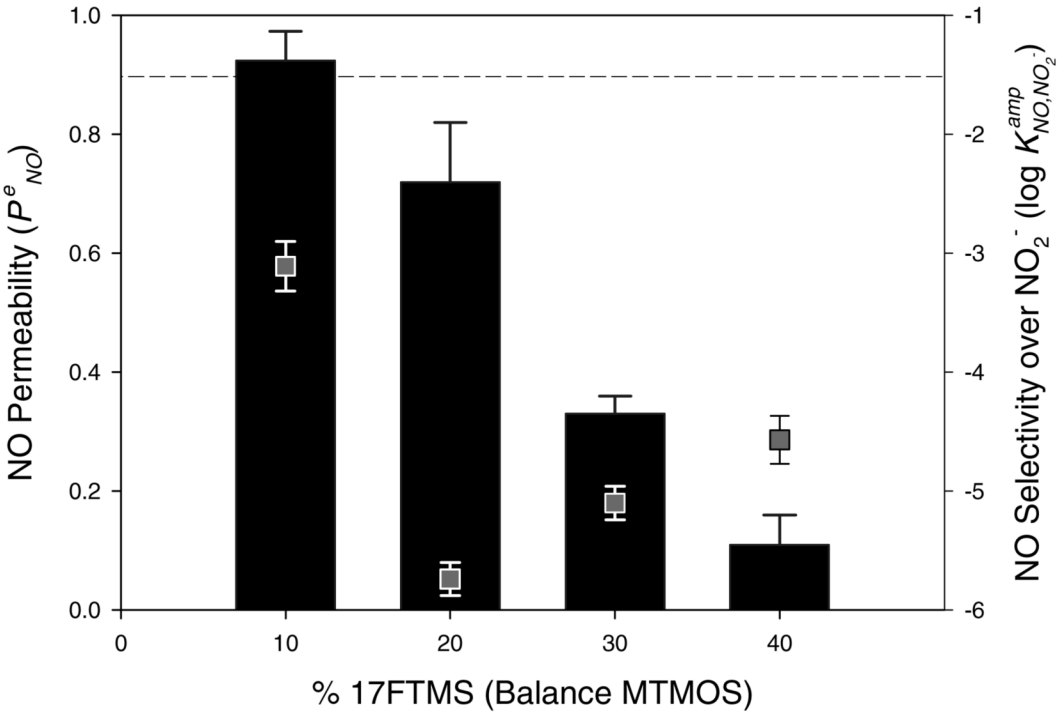

Figure 6.

NO permeability (bar graphs, left axis) and selectivity over nitrite (scatter plots, right axis) as a function of the concentration of 17FTMS (balance MTMOS). All xerogels were synthesized under acid-catalyzed conditions. The dashed line indicates NO selectivity for the bare Pt electrode over nitrite. Data are represented as means ± SD (*n* is at least 3).

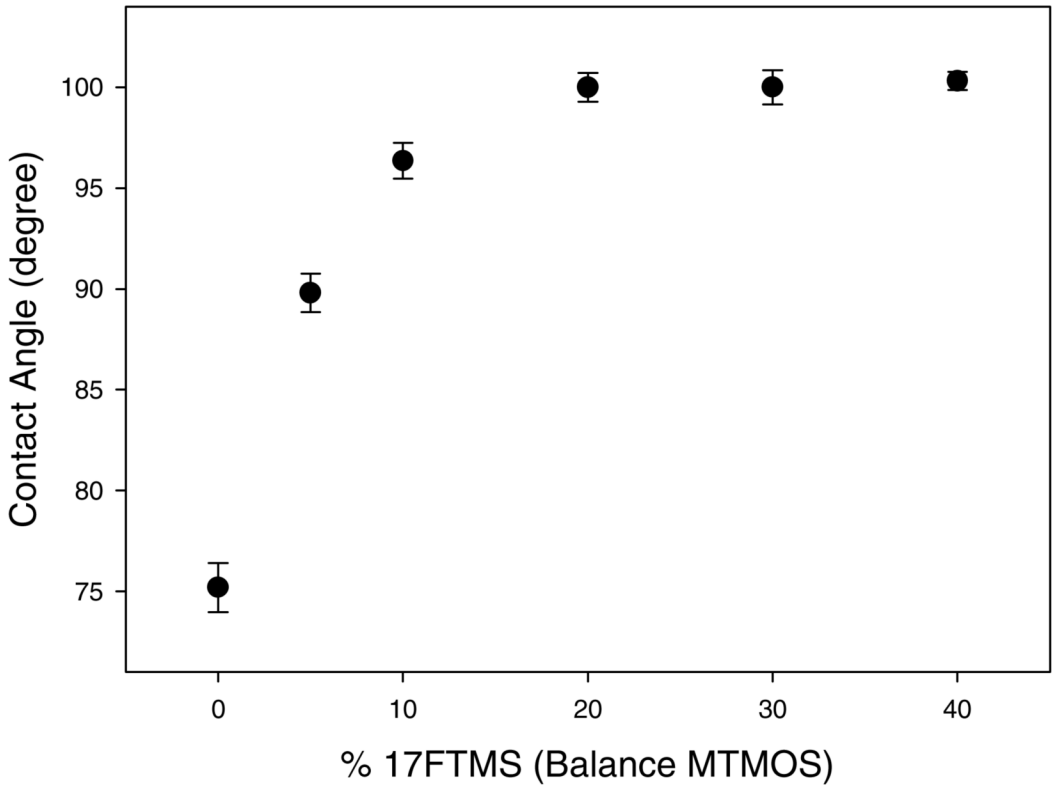

Figure 7.
Static water contact angles as a function of the concentration of 17FTMS (balance MTMOS). All xerogels were synthesized under acid-catalyzed conditions. Data are represented as means ± SD (n = 15).

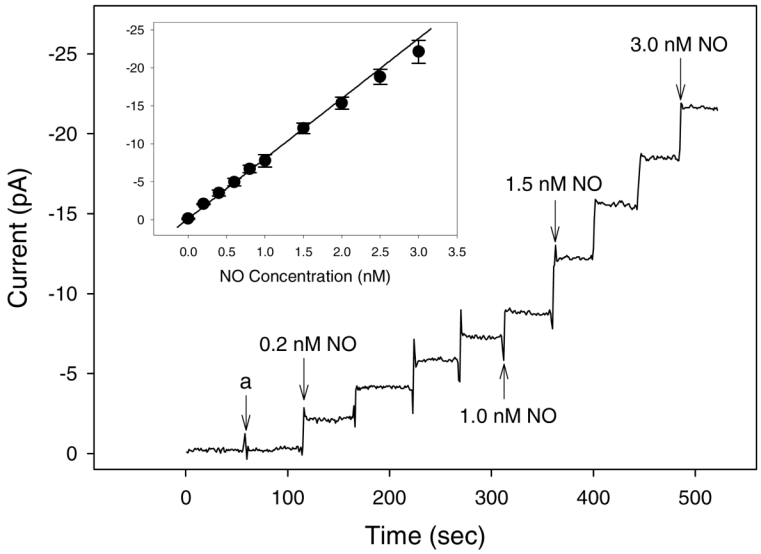

Figure 8.

Dynamic response to NO and interfering species. Inset: calibration curve of the NO-selective microelectrodes coated with 20% 17FTMS/MTMOS xerogels prepared via acid catalysis. (a) injection of 100 mM each of nitrite, ascorbic acid, uric acid, acetaminophen, dopamine, and ammonia/ammonium. Data are represented as means ± SD (*n* = 3).

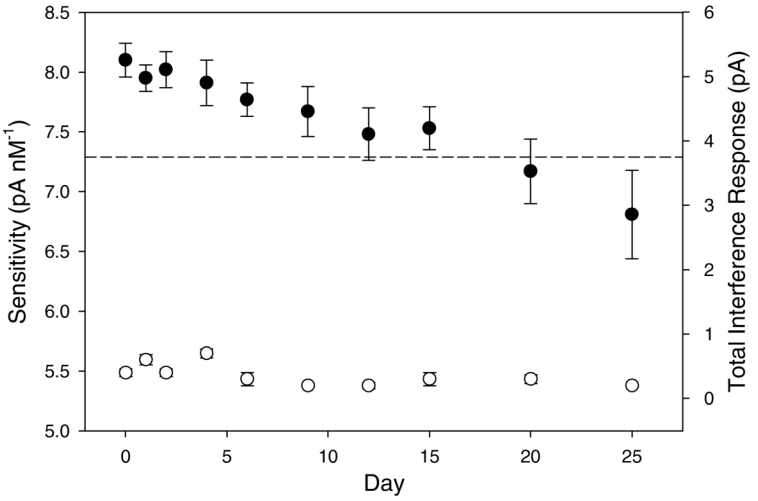

Figure 9.

Amperometric response to NO (•, left axis) and interfering species (○, right axis) determined from 0.2 to 3.0 nM NO and 100 μM each of nitrite, ascorbic acid, uric acid, acetaminophen, dopamine, and ammonia/ammonium, respectively. The platinized Pt/W microelectrodes were modified with 20% 17FTMS/MTMOS. Sensors were stored in PBS (0.01M, pH 7.4) between measurements at room temperature. The dashed line indicates 90% of the sensor's initial sensitivity. Data are represented as means ± SD (*n* is at least 3).

Table 1

Electrochemical characteristics of NO sensors modified with 20% 17FTMS/MTMOS xerogel membranes synthesized under different catalytic conditions[a,b,c]

catalytic condition	permeability, P_i^e		permselectivity, α_{NO,NO_2^-}	selectivity,[d] $\log K^{amp}_{NO,NO_2^-}$
	i = NO	$i = NO_2^-$		
control[e]	0.75 ± 0.06	0.0091 ± 0.0010	83 ± 11	−3.21 ± 0.15
6.5 mM HCl[f]	0.72 ± 0.09	<0.0001	7200 ± 900	−5.74 ± 0.14
6.5 mM NaOH[f]	0.13 ± 0.02	<0.0001	1300 ± 200	−4.83 ± 0.09

[a] The data are represented as means ± SD (n = 3 or 5).

[b] Xerogel composition used: 60 μL of MTMOS, 15 μL of 17FTMS (20%, balance MTMOS), 300 μL of ethanol, and 80 μL of water. All fluorinated xerogel coatings were dried under ambient conditions for 24 h.

[c] Values were determined at 10 μM of NO and 100 μM of NO_2^- in deoxy-genated PBS (0.01 M, pH 7.4), respectively.

[d] To determine selectivity, the separate solution method was employed.

[e] Composition without a catalyst.

[f] The addition of 5 μL of 0.5 M HCl or 0.5 M NaOH in the above xerogel composition, respectively.

Table 2

Stability of 20% 17FTMS/MTMOS xerogels prepared via acid catalysis[a,b]

xerogel composition	xerogel fragmentation, Si (μmol·cm^{-2})				
	7d	14 d	21 d	28 d	42 d
20% 17FTMS/MTMOS[c]	< 0.04[d]	< 0.04[d]	0.11 ± 0.03	0.17 ± 0.10	0.20 ± 0.08

[a] Number of samples: n = 15.

[b] Values were determined via DCP-OES.

[c] Xerogel composition: 60 μL of MTMOS, 15 μL of 17FTMS (20%, balance MTMOS), 300 μL of ethanol, 80 μL of water, and 5 μL of 0.5 M HCl. The fluorinated xerogel films were dried under ambient conditions for 24 h, and soaked in PBS (0.01 M, pH 7.4) at room temperature for 1 to 6 weeks.

[d] Values obtained were under the detection limit of the instrument.